Talanta 165 (2017) 274–281

Contents lists available at ScienceDirect

Talanta

journal homepage: www.elsevier.com/locate/talanta

A label–free GR–5DNAzyme sensor for lead ions detection based on nanoporous gold and anionic intercalator

Yaoyu Zhou[a], Jiachao Zhang[a], Lin Tang[b,*], Bo Peng[b], Guangming Zeng[b,*], Lin Luo[a], Jun Gao[a], Ya Pang[c], Yaocheng Deng[b], Fengfeng Zhang[a]

[a] College of Resources and Environment, Hunan Agricultural University, Changsha 410128, China
[b] College of Environmental Science and Engineering, Key Laboratory of Environmental Biology and Pollution Control, Ministry of Education, Hunan University, Changsha 410082, China
[c] Department of Biotechnology and Environmental Science, Changsha College, Changsha 410003, China

ARTICLE INFO

Keywords:
Label–free
Lead
Anionic intercalator
GR–5DNAzyme
Nanoporous gold

ABSTRACT

A label–free electrochemical sensor, based on a classic lead ions (Pb^{2+})–dependent GR–5DNAzyme as the catalytic unit, disodium–anthraquinone–2,6–disulfonate (AQDS) as DNA intercalator, and nanoporous gold (NPG) for signal amplification, was designed for sensitive and selective detection of Pb^{2+}. Firstly, NPG modified electrode surface were employed as a platform for the immobilization of thiolated probe DNA, and then, hybridized with DNAzyme catalytic beacons. The Pb^{2+}–induced catalytic reaction makes the substrate strand break at the cleavage sitGe irreversibly, which disturbs the formation of DNA strands. AQDS served as an indicator that intercalated into the base–pairing regions of DNAzyme, resulting in a strong electrochemical signal. In the presence of Pb^{2+}, the complementary regions were reduced, due to the fracture of the DNA strand, resulting in the release of AQDS. And a decreased current was obtained, corresponding to Pb^{2+} concentration. Taking advantage of the amplification effect of NPG electrode for increasing the reaction sites of thiol modified capture probe, the proposed electrochemical biosensor could detect Pb^{2+} quantitatively, in the range of 1–120 nM, with a limit of detection as low as 0.02 nM, which is much lower than the maximum contamination level for Pb^{2+} in drinking water defined by the U.S. Environmental Protection Agency. The electrochemical sensor was also used to detect Pb^{2+} from real water samples, and the results showed excellent agreement with the values determined by inductively coupled plasma mass spectroscopy. This biosensor showed a promising potential for on–site detecting Pb^{2+} in aqueous environment.

1. Introduction

Lead ions (Pb^{2+}) is an important pollutant mainly arising from lead–based paints and contaminated water, soils and foodstuffs [1,2]. Lead causes adverse health effects in human bodies, including neurological, cardiovascular, reproductive, and developmental disorders [3–5]. The maximum contamination level (MCL) for Pb^{2+} in drinking water is 72 nM according to the U.S. Environmental Protection Agency (EPA). In fact, even lower than 72 nM of Pb^{2+} is associated with children's neuro–developmental deficits [6–9]. Hence, it is of great significance to monitor its level in the environment.

Traditional quantitative methods, such as atomic absorption spectrometry (AAS) [10], and inductively coupled plasma mass spectroscopy (ICP–MS) [11], are the standard techniques utilized for Pb^{2+} determination. However, these methods need expensive and complex equipment, materials and include time consuming extraction steps to eliminate the excipients, contaminants and interfering ions [12]. Besides, traditional methods cannot be used as portable devices for on–site/in–site quantification, and meanwhile large–scale determination of heavy metals can be time consuming, labor intensive and costly. In contrast, electrochemical techniques have great potential for on–site/in–site detection of multiple heavy metals. Anodic stripping voltammetry (ASV) has been considered to be the most effective tool for the direct electrochemical detection of trace Pb^{2+} ions due to an effective pre-concentration step followed by electrochemical stripping measurements of the accumulated analytes [13–15]. However, the task for sensor to avoid interferences from complex environmental matrices is very hard.

Recently, many biochemical and biophysical studies have been carried out on DNAzymes. Important insights have been gained regarding metal binding sites, metal–dependent activity, and catalytic mechanisms for these DNAzymes. One of the most significant practical

* Corresponding authors.
E-mail addresses: tanglin@hnu.edu.cn (L. Tang), zgming@hnu.edu.cn (G. Zeng).

http://dx.doi.org/10.1016/j.talanta.2016.12.069
Received 10 October 2016; Received in revised form 19 December 2016; Accepted 24 December 2016
Available online 25 December 2016
0039-9140/

applications for DNAzymes is metal ion detection due to their high metal ion selectivity (avoid interferences from complex environmental matrices), such as the reported DNAzyme for Pb^{2+} is about 40,000–fold selective [16] over other competing metal ions, and the DNAzyme for UO_2^{2+} is more than 1,000,000–fold selective over other competing metal ions [17]. This kind of metal selectivity can be found in many other DNAzymes. Therefore, DNAzymes have been converted into sensors for a wide range of metal ions such as mercury(Hg^{2+}) [18], lead(Pb^{2+}) [19], uranyl(UO_2^{2+}) [20], magnesium(Mg^{2+}) [21], zinc(Zn^{2+}) [22], copper(Cu^{2+}) [23], calcium(Ca^{2+}) [24], silver(Ag^{+}) [25], and thallium(Tl^{3+}) [26]. Moreover, it is noteworthy that Liu's group found a series of metal ions–based DNAzymes, and elucidated the relationship between metal ion selectivity and DNAzyme sequence and structure in these systems [24–27]. These discoveries help to find and select the target metal ions–based DNAzyme, and contributed to the mental ions biosensor based DNAzyme. In addition, it has been found that 8–17DNAzyme and GR–5DNAzyme have the highest activity with Pb^{2+} and are by far the fastest RNA–cleaving DNAzymes. GR–5 reacts only with Pb^{2+} while 17E is also active with a number of other divalent metal ions [28]. Hence, GR–5DNAzyme was selected in this work.

Besides, in developing highly sensitive electrochemical sensors, amplified detection strategy is the central research topic. In recent years, various nanomaterials (e.g., graphene oxide, mesoporous carbon, carbon nanotubes, metal nanoparticles, quantum dots, magnetic nanoparticles, etc.) were employed as DNA immobilization substrates and recognition elements in biosensors [29–35]. These nanomaterials with large surface area, abundant binding sites, excellent biocompatibility and a synergic effect among conductivity, are beneficial to increase the amount of the immobilized DNA probe significantly, and thus, the amplified electrochemical detection signals are obtained. In our earlier studies, a novel label–free impedimetric sensing system was proposed for the detection of Pb^{2+} based on ordered mesoporous carbon–gold nanoparticle, and the detection limit of was 0.2 nm [32]. In addition, we also developed a DNA biosensor based on carboxylic acid group functionalized multiwalled carbon nanotubes and gold nanoparticles (GNPs) for the quantification of lead ions [36], and the detection limit of 0.0043 pM is much lower than the EPA limit of Pb^{2+} in drinking water [37]. These detecting systems are highly sensitive and selective at the cost of multiple assembly steps and multiple signal amplification, which may affect the operability of the biosensors. Moreover, in our previous work, we have also demonstrated new and simple strategies to increase the electrochemical signals and lower the detection limits using nanoporous gold (NPG) with the controllable three–dimensional nanoporous metal film and simple preparation as the platform for nucleotide immobilization [38,39]. Hence, based on our previous efforts, NPG was applied to fix DNA, and as a transducer to convert the recognition information into a detectable signal.

Besides, the choice of signal agent is also important for the DNA–based biosensors. It is well known that the indicators are classified into cationic and anionic intercalators, both single strand probe DNA (ssDNA) and double strands probe DNA (dsDNA) carry negative charges. Hence, there was large background signal of DNA–based biosensors using anionic intercalators because of the electrostatic attraction. In previous work, Zhang et al. introduced that employing the cationic intercalators of hexaammineruthenium(III) chloride (RuHex) as indicators may increase background signal, and oligonucleotide-functionalized gold nanoparticles as amplifying tags may cause blocking phenomenon in NPG based electrode [39]. Alternatively, anionic intercalators can reduce background signal. A comparison of anionic and cationic intercalators for the electrochemical transduction of DNA hybridization was studied as reported by Wong and coworkers [40]. They found that disodium–anthraquinone–2, 6–disulfonate (AQDS), a kind of anionic intercalators, can intercalate into the dsDNA but not into ssDNA, when only the ssDNA was present on the interface, there was no background electrochemical signal [40]. Thus, AQDS was used as the electroactive indicator in this work in order to improve the sensitivity, lower background signal.

Herein, the aim of this work was to develop a simple biosensor with sensitivity and selectivity for the quantification of Pb^{2+} based on GR–5DNAzyme, NPG and AQDS. This strategy for Pb^{2+} quantification is highly accurate, relatively simple to operate, and to exploit strong resistance of the sensor to environmental impact disturbance. NPG was carefully coated onto a pretreated electrode via physical adsorption, and then modified with Pb^{2+}–DNAzyme. AQDS was selected as an electroactive signal indicator. Furthermore, Pb^{2+} detections in landfill leachate and tap water samples are performed to demonstrate the practical use of this sensor. The developed sensor with high sensitivity and selectivity may be an alternative method for Pb^{2+} ion detection in environmental, biomedical, and other applications.

2. Experimental

2.1. Chemicals and reagents

Disodium–anthraquinone–2, 6–disulfonate was purchased from TokyoChemical Industry Co., Ltd. (Tokyo, Japan). Tris (2–carboxyethyl) phosphinehydrochloride (TCEP), 6–mercaptohexanol (MCH) and tris–(hydroxymethyl) aminomethane were purchased from Sigma–Aldrich (USA). $Pb(NO_3)_2$, $K_3Fe(CN)_6$, $K_4Fe(CN)_6$, and all aqueous solutions were prepared using ultrapure water (18.2 MΩ·cm, Milli–Q, Millipore). 50 mM tris–acetate buffer (pH 8.0) containing 300 mM NaCl and phosphate buffer saline (PBS, 0.15 M KH_2PO_4 and 0.15 M Na_2HPO_4) were used in this work. All oligonucleotides used in our experiment were synthesized and high performance liquid chromatography (HPLC)–purified by Sangon Biotech. Co., Ltd. (Shanghai, China). Their base sequences are as follows: 5′–SH–C_6–ACAGACATCATCTCTGAAGTAGCGCCGCCGTATAGTGAG–3′ (S1, capture probe) and 5′–CTCACTATArGGAAGAGATGATGTCTGT–3′ (S2, a complementary substrate oligonucleotide of the DNAzyme which contains a single, scissile ribo–adenine) [28]. Probes were dissolved in 50 mM tris–acetate buffer (pH 8.0) containing 300 mM NaCl and kept at −20 °C for further use. Phosphate buffer saline (pH 7.0) containing 0.2 M NaCl was used to store the 1 mM AQDS, in the dark. NPG was prepared according to our previous method. Briefly, Au/Ag alloy leaf was sandwiched between two supporting papers, and cut into small pieces of any size, subsequently, floated onto concentrated nitric acid for dealloying about 1 h and then water for rinsing 3 times [38,41].

2.2. Apparatus

All electrochemical measurements, such as cyclic voltammograms (CVs), electrochemical impedance spectroscopy (EIS) and different pulse voltammetric (DPV), were performed in aconventional three–electrode cell at room temperature with a CHI760D electrochemical workstation (Chenhua Instrument Shanghai Co., Ltd., China). A model pHSJ–3 digital acidimeter (Shanghai Leici Factory, China) was used to measure the solution pH. A Sigma 4K15 laboratory centrifuge, a vacuum freezing dryer and a mechanical vibrator were used in the assay.

2.3. Sensor fabrication and detection process

Probe was activated by 2 mM TCEP (which isincluded to reduce disulfide bonded oligomers), and diluted by 50 mM tris–acetate buffer (pH 8.0). The bare glass carbon electrode (GCE) was polished in alumina slurry firstly, and then rinsed with deionized water. Finally, the electrode surface was treated by H_2SO_4 (0.5 M) with cyclic voltammetry scan (between 0 and 1.2 V at the scan rate of 50 mV s^{-1}) until a reproducible scan was obtained. After being dried, the nanoporous gold (prepared by selective dissolution of Ag from Ag/Au) was carefully coated onto a pretreated GCE via physical adsorption, and then, washed with ultrapure water to neutral pH [38].

Subsequently, the mixture solution (7 μL S1, 50 mM tris–acetate buffer (pH 8.0), and 1 mM TCEP (which is included to reduce disulfide bonded oligomers) was dropped onto the electrode surface for self–assembling through Au–S bonding for 12 h in 4 °C. The probes of this biosensor were hybridized as follows. 6–mercapto–1–hexanol (MCH) solution (400 μL, 1 mM) was used to immerse the modified electrode with S1 probes for 1 h to improve the stability and quality, to reduce nonspecific adsorption of DNA and to obtain a well aligned DNA monolayer. Then, the electrode was soaked in the solution with S2, and incubated at room temperature for 70 min to yield the final GR–5DNAzyme assembly on the surface. Subsequently, the electrode was immersed in buffer (50 mM Tris–acetate, 0.2 M NaCl, pH 8.0) to reduce the nonspecific adsorption of S2. And then the electrode was immersed into AQDS solution.

For Pb^{2+} detection, the DNA–modified electrode surface was then allowed to react with various concentrations of target Pb^{2+} in the buffer (50 mM Tris–acetate, 0.2 M NaCl, pH 8.0) for 60 min in a 40 °C water bath to obtain the maximum cleavage of substrate strand on the modified electrode. Then the electrode was removed from the buffer, and allowed to cool down to room temperature within 1 h. Finally, a CHI760D electrochemical workstation was used, and all the measurements were carried out at room temperature with conventional three–electrode system. The modified electrode was treated with various concentrations of Pb^{2+} in buffers (50 mM tris–acetate, 0.2 M NaCl, pH 8.0) for 2 h. Subsequently, it was washed with tris–acetate buffer (pH=8.0). EIS and CVs were performed in 0.15 M PBS (pH 7.0) containing 10 mM KCl and 5 mM $Fe(CN)_6^{3-/4-}$ (1:1). Besides, the electrochemical current was measured using different pulse voltammetric (DPV) by the PBS (pH 7.0) containing addition of 0.3 M NaCl. And the DPV measurements were performed from −700 to −300 mV with pulse amplitude of 50 mV and width of 50 s. The data for condition optimization and the calibration curve were the average values of three measurements.

2.4. Analysis of environmental samples

As a further step, we attempted to prove the general applicability of this sensor to practical samples including tap water and landfill leachate sample. Tap water samples were obtained from Changsha Running–water Company, China. And landfill leachate was obtained from municipal solid waste landfills in Changsha, China. All the environmental samples were first centrifuged at 12,000 rpm for 20 min and then filtered through a 0.2 mM membrane to remove oils and other organic impurities, the samples were spiked with standard solutions of Pb^{2+} prior to measurement using the proposed method and ICP/MS.

3. Results and discussion

3.1. Characteristics of the electrode

Apart from excellent biocompatibility, NPG with porous structure is a suitable candidate for fabricating DNA–based biosensors because its large surface area can realize significantly amplified detection, and the surface area and average pore size estimate were about 9.42 $m^2\ g^{-1}$ and 45.7 nm [38,39]. In this work, NPG was prepared from dealloying corrosion of Ag/Au alloy, and then coated onto GCE via physical adsorption. As seen in Fig. 1, the NPG film with spatial arrangement of pores and controllable size was modified on the GCE surface successfully. The total active surface of NPG film was significantly enhanced about 9.4–fold compared with the GCE according to our previous work, due to the NPG electrode possesses a total active surface of 184.6 mm^2, while that of the bare GCE electrode is 19.6 mm^2 [38], representing a much larger surface area and more reaction sites of the Au–based porous electrode.

Besides, to test the performance of the modified electrode, cyclic voltammograms (CV) was carried out in phosphate buffer (containing

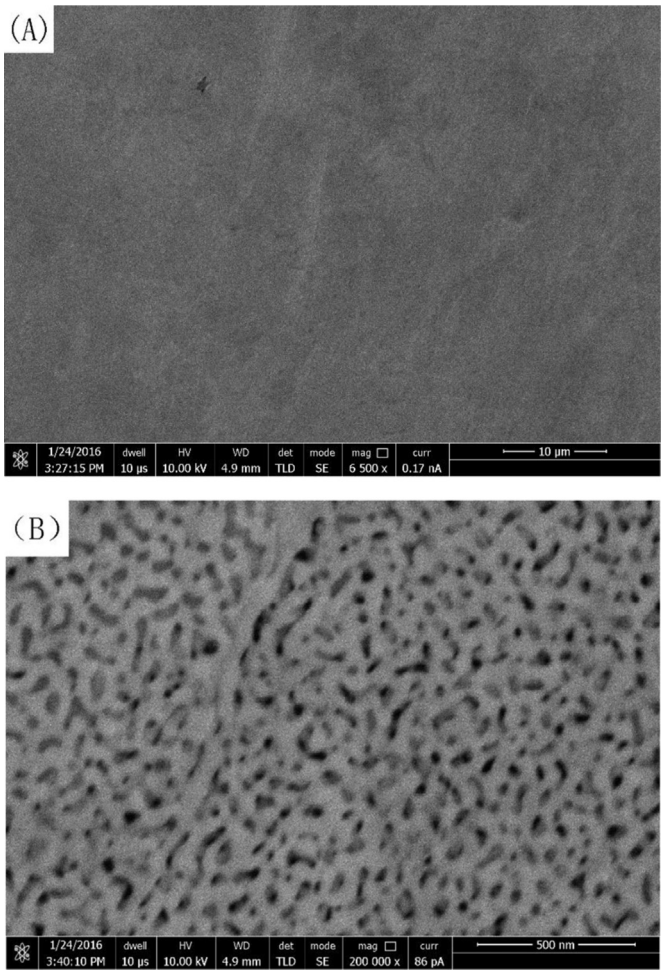

Fig. 1. The SEM images of NPG (A image scale of 10 μm), NPG (B, image scale of 500 nm).

5 mM $Fe(CN)_6^{3-/4-}$ (1:1) and 10 mM KCl, pH 7.4). As seen in Fig. S–1A, the peak current of the redox probe was increased after the immobilization of NPG on the GCE, indicating that the NPG/GCE had a good current response capability. Correspondingly, EIS showed that the impedance of the NPGs/GCE and bare GCE in phosphate buffer. As seen in Fig. S-1B, an obvious large interfacial resistance was observed from the GCE, and the R_{CT} value was about 684.9 Ω. However, an almost straight line was observed with NPG assembled, and the electron–transfer resistance (R_{CT}) value was about 34.15 Ω (as seen in Table S–1), which indicated that the introduction of NPG could enhance the electron transfer kinetics to a large extent. What's more, the electron transfer ability of the modified electrode reflected by EIS was in accordance with the current density response reflected by CV.

3.2. Experimental principle and sensing scheme

A succinct strategy was designed to detect Pb^{2+} ions using the prepared electrode (Fig. 2). The single strand oligonucleotide S1 with Au–S covalent bond acting as an anchor substrate on the composite platform was ready for the reconstitution of the S2 to form a stable structure. And then the electrode was immersed into AQDS solution for electrochemical detection. AQDS has a unique anthracene ring structure, can intercalate into the structure of dsDNA, and exhibits a reversible 2–electron transfer process for its quinone/hydroquinone redox couple in electrochemistry.

However, once in the presence of Pb^{2+}, the trans–acting catalytic strand cleaved the sessile phosphodiester of the substrate into two fragments, leading to the decreased AQDS intercalate into the structure

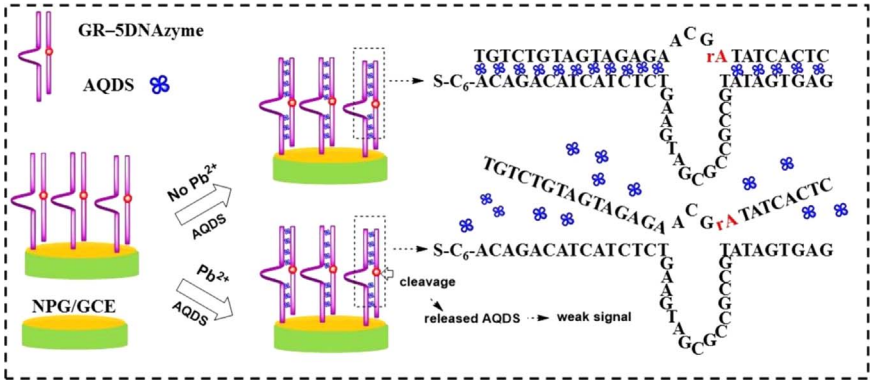

Fig. 2. A self–assembly method and mechanism of this sensor.

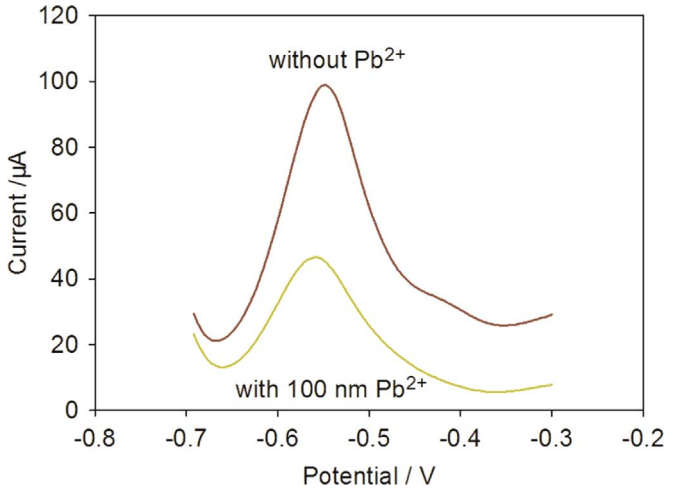

Fig. 3. Different pulse voltammetric measurement from −700 to −300 mV under a pulse amplitude of 50 mV and width of 50 s in 10 mL of PBS containing 0.2 M NaCl (pH 7.0), after reacting with 0 nM and 100 nM Pb^{2+} ion for 60 min and then immersing into AQDS solution containing 0.2 M NaCl for 300 min.

of dsDNA. Therefore, the decrease of AQDS attached on the electrode surface, leading to the decrease of the electrochemical signal. As seen in Fig. 3, the DPV curves with biosensor in the presence and absence of Pb^{2+} ions. After addition of Pb^{2+}(100.0 nM), the electrochemical signal decreased significantly. In fact, the changes of DPV signal in the presence and absence of the metal ion were different and dependent on the concentration of the given metal ion. On the basis of the results discussed above, the interactions between DNA and Pb^{2+} led to the decreased DPV signal, which was used for the detection of Pb^{2+}.

3.3. Optimization of the variables of experimental conditions

The experimental conditions were optimized before the quantitative analysis of Pb^{2+}. Fig. 4A showed the effect of self–assembly time of capture probe (S1) on the modified electrode surface. The Δ*I*increased with the self–assembly time, and then reached a plateau at 12 h. Therefore, the self–assembly time of 12 h was used in the subsequent measurements. Similarly, the optimization of hybridization conditions includes hybridization time of DNAzyme hybridization (S2) reaction. The hybridization time is an important factor to ensure the adequacy of a contact reaction. The response current increased sharply with the hybridization time increasing from 30 to 60 min, then leveling off (Fig. 4B). The reaction time between DNA with Pb^{2+} would have profound effect on the performance of the biosensor. Upon exposure to 100.0 nM Pb^{2+}, the Δ*I*increased with 60 min of incubation and then remained constant when the action time was further elongated (Fig. 4C). So, an incubation time of 60 min was employed as the optimum reaction time between DNA with Pb^{2+}. The effect of reaction temperature on the response of the system is also investigated. Fig. 4D depicts the Δ*I*response of the sensor at varying reaction temperature ranging from 25 to 50 °C. It is observed that the peak current increases with the temperature from 25 to 40 °C and then decreases rapidly as the reaction temperature increases from 40 to 50 °C. Thus, 40 °C is chosen as the optimized reaction temperature. And the sensor was immersed in AQDS solution containing 0.2 M of NaCl for 360 min [38].

3.4. Quantification of Pb^{2+} concentration

According to the above standard procedures and under the optimized assay conditions, the DPV was used to record the current of various Pb^{2+} concentrations with the biosensor, and the results are shown in Fig. 5. The various concentrations of Pb^{2+} were 0, 0.05, 0.1, 1.0, 20, 40.0, 60.0, 80.0, 100.0 and 120.0 nM. The experimental results were shown in Fig. 5A. From this figure, it can be observed that the current of AQDS decreases gradually with increases of the concentration of Pb^{2+}. Besides, it is linear with the concentration of the complementary Pb^{2+} from 1.0 to 120.0 nM. The linear regression equation was $Y=(-0.35839 \pm 0.0142)X + (81.19795 \pm 1.09951)$ (Y is the current (uA), X is the value of the target concentration (nM)) with a correlation coefficient $R^2=0.99065$. The detection limit of the biosensor was estimated to be 0.02 nM, based on signal/noise ratio=3. The Pb^{2+} detection performances of the proposed sensor were compared with other previously reported sensors, and the results are listed in Table 1. Compared to the sensors based on DNAzyme, this sensor showed a relatively wide linear range, and the limit of detection was competitive with other highly sensitive detection approaches, such as fluorescence, surface enhanced raman scattering, colorimetry and electrochemical methods. Besides, compared to the sensors based on diamond without DNAzyme, this sensor showed a comparable property in linear range and detection limit.

3.5. Repeatability and stability the biosensor

Repeatability is also an important issue for sensors. In the present study, the sensing interface could be easily repeatability by the same biosensor for 100.0 nM Pb^{2+}. It was found that the sensor has good repeatability, and could be used more than two times without significant loss of its original sensing efficiency (Fig. 6). The stability of the biosensor was also explored. We also investigated the stability of this sensor through the response to 100.0 nM Pb^{2+} for 1 month (as shown in Fig. S–2A). Beyond this period, the experiment was carried out per 5 days and 10 days. When not in use, the electrode was stored in a moist state at 4 °C. The result showed that the biosensor retained about 81% of its original Δ*I*after 1 month. The result indicated that this biosensor has relatively good stability, and the reason might be that the DNAzyme–based sensor is sensitively responsive to its target ion.

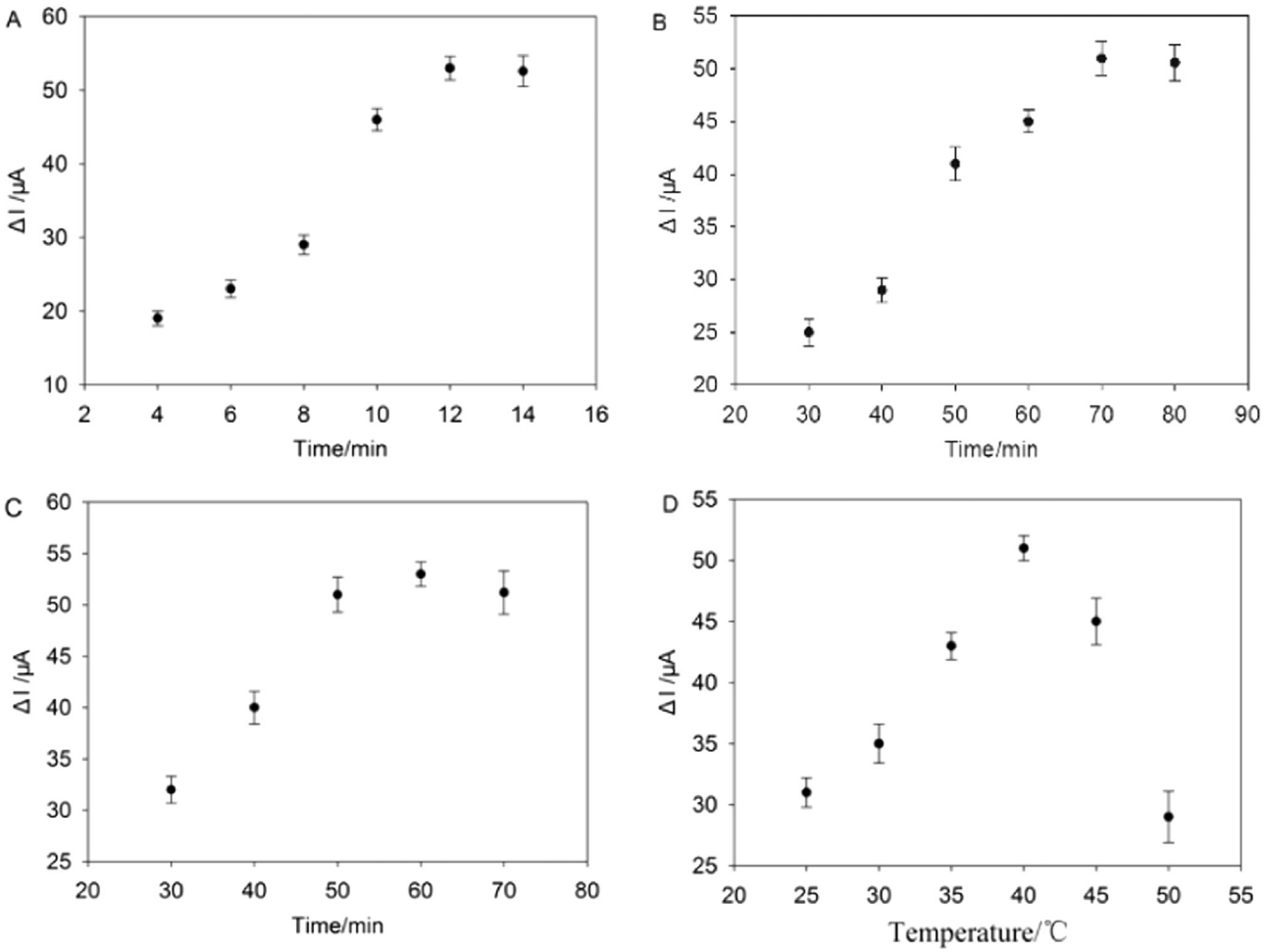

Fig. 4. Optimization of experimental conditions: (A) effect of self–assembly time (capture probe); (B) effect of hybridization time; (C) the time–course of the Pb^{2+} hybridized with DNAzyme; (D) experiment temperature, upon exposure to 100 nM Pb^{2+}. All tested electrodes were fabricated by immobilizing 10 μL capture probe on electrodes surfaces at 4 °C. Error bars indicate standard deviations from three replicative tests.

3.6. The reproducibility and selectivity of the biosensor

The reproducibility of this biosensor was investigated. Six biosensors were fabricated with five different GCEs by the same steps independently, and used to detect 100.0 nM Pb^{2+}, as presented in Fig. S–2B. The RSD was 4.9% with five biosensors prepared independently, indicating that the fabrication procedure was reliable, and this biosensor had good reproducibility.

The sensing interfaces were determined with various competing divalent metal ions which are commonly present in real samples, such as Ca^{2+}, Zn^{2+}, Mn^{2+}, Hg^{2+}, Co^{2+}, Cu^{2+}, Cd^{2+}, to verify the selectivity of this approach for the detection of Pb^{2+} in practical applications. Under the optimal experimental conditions, 100.0 nM of Pb^{2+}, 1000.0 nM of Ca^{2+}, Zn^{2+}, Mn^{2+}, Hg^{2+}, Co^{2+}, Cu^{2+}, Cd^{2+}, and their mixture containing 100.0 nM of Pb^{2+}, and their mixture without Pb^{2+} were respectively measured (Fig. 7). The degree of interference was calculated by the following method [31,51]:

$$\tau = \frac{\Delta I}{I_0} = \frac{I_0 - I_x}{I_0} \quad (1)$$

where τ is the percent of interference; I_0 and I_x stands for the response currents without and with different concentrations of Pb^{2+}, respectively. As seen in Fig. 7 and Table S–2, negligible signal response (< 3.6%) was observed upon the addition of other tested ions, and on the contrary, significant response of ΔIas observed for Pb^{2+}. Hence, the results showed excellent selectivity toward Pb^{2+} over other ions due to a specificity of GR–5DNAzyme for Pb^{2+} ion. Second, Pb^{2+} and other ions were mixed to form a mixture solution as a sample for the anti–jamming capability testing of this sensor (Fig. 7). The $\Delta I$was obviously higher than other samples without Pb^{2+}. These results clearly indicated that the approach is not only insensitive to other ions but also selective toward Pb^{2+} in their presence. As noted above, the present sensor had excellent selectivity and anti–jamming capability.

3.7. Real samples detection

To evaluate the practicality of the present method, several environmental water samples spiked with Pb^{2+}, with concentrations of 0, 5.0, 50.0 and 100.0 nM, were tested using the proposed method and ICP/MS. The environmental water samples used in the study were tap water and landfill leachate samples. All the samples were filtered through a 0.2 μm membrane and then centrifuged for 20 min at 12,000 rpm before the detection measurements were performed. The concentrations of total Pb^{2+} in water samples were measured by proposed method and ICP/MS. The results were summarized in Table 2, and presented excellent agreement with the found values quantified by ICP/MS, suggesting good accuracy and precision of the proposed method for Pb^{2+} quantification in real samples. Although this work here demonstrated the quantification of Pb^{2+} ions only, the proposed sensing strategy can in principle be used to detect different analytes (other metal ions or DNA) using other specificity structures that selectively bind the other analytes.

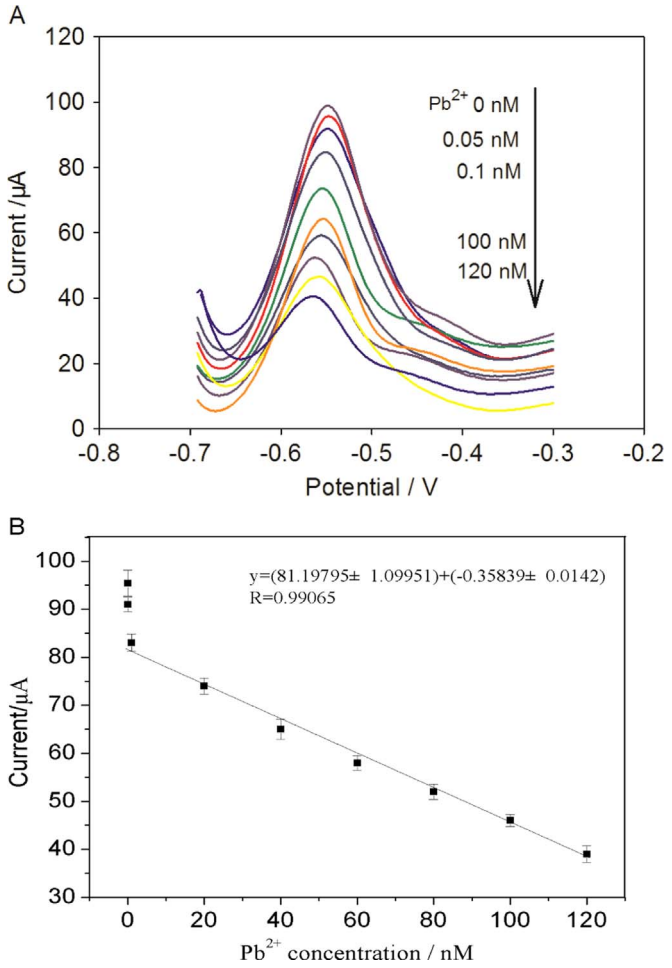

Fig. 5. (A) DPV curves after the addition of various concentrations (0–120 nM) of Pb^{2+} in pure hybridization buffer. (B) Linear relationship between the current and Pb^{2+} concentration in buffer. The concentrations of Pb^{2+} were 1.0, 20.0, 40.0, 60.0, 80.0, 100 and 120 nM. Every data point was the mean of three measurements. The error bars are the standard deviation.

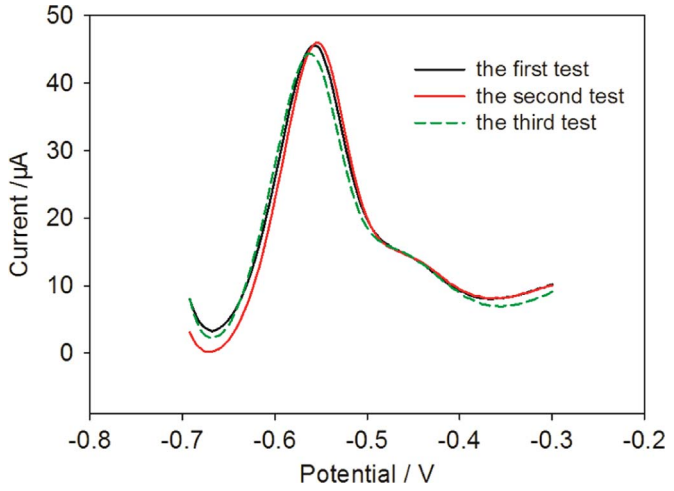

Fig. 6. The repeatability of the same biosensor for 100 nM Pb^{2+}(different line represents different testing sample with the same biosensor).

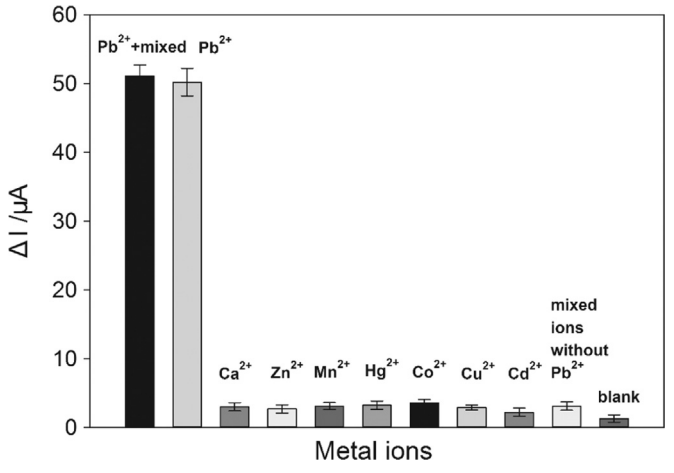

Fig. 7. Selectivity and interference study in the analysis of Pb^{2+} by the DNA system. The data were averages of three replicate measurements.

Table 1
Comparison with other published Pb^{2+} detection sensor.

Lead sensor	Materials	Linear range (mol L^{-1})	LOD (mol L^{-1})	References
Electrochemical detection/8–17DNAzyme	OMC–GNPs	5.0×10^{-10}– 5.0×10^{-5}	2.0×10^{-10}	[32]
Electrochemical detection/8–17DNAzyme	GNPs	1.0×10^{-10}– 3.5×10^{-8}	2.8×10^{-11}	[37]
Electrochemical detection/8–17DNAzyme	Magnet–controlled electronic switch	1.0×10^{-10}–7.5×10^{-8}	3.7×10^{-11}	[42]
Electrochemical detection/8–17DNAzyme	GNPs	5.0×10^{-9}–1.0×10^{-7}	1.0×10^{-9}	[43]
Electrochemical detection/8–17DNAzyme	QDs	1.0×10^{-9}–1.0×10^{-6}	6.0×10^{-10}	[44]
SERS/8–17DNAzyme	GNPs	2.0×10^{-8}–1.0×10^{-6}	2.0×10^{-8}	[45]
Colorimetric detection/ 8–17DNAzyme	GNPs	2.5×10^{-8}–3.0×10^{-7}	2.0×10^{-8}	[46]
Fluorescencedetection/ 8–17DNAzyme	Magnetic beads	1.0×10^{-9}–1.0×10^{-7}	6.0×10^{-10}	[47]
Fluorescence detection/ GR–5DNAzyme	Microarray	1.0×10^{-9}–1.0×10^{-6}	1.0×10^{-9}	[48]
Electrochemical detection	Natural diamond	1.0×10^{-9}–1.0×10^{-6}	1.0×10^{-10}	[49]
	Synthetic diamond (50 μm)	1.0×10^{-10}–1.0×10^{-7}	1.0×10^{-11}	
without DNAzyme	Synthetic diamond (1 μm)	1.0×10^{-10}–1.0×10^{-8}	1.0×10^{-11}	
Electrochemical detection without DNAzyme	ErGO–GRC	2.5×10^{-10}–2.0×10^{-9}	9.0×10^{-11}	[50]
Electrochemical detection/GR–5DNAzyme	NPG	1.0×10^{-9}–1.2×10^{-7}	2.0×10^{-11}	This work

Abbreviations: OMC–GNPs, Ordered mesoporous carbon–gold nanoparticles; QDs, quantum dots; SERS, Surface enhanced raman scattering; ErGO–GRC, Electrochemically reduced graphene oxide–graphite reinforced carbon.

Table 2
Determination of Pb^{2+} in real samples.

Sample	Added Pb^{2+}(nM)	Proposed method[a] (nM)	ICP/MS[a] (nM)	RSD (%)[b]
Tap water 1	0	c	c	–
Tap water 2	5.0	5.12	5.02	1.39
Tap water 3	50.0	51.03	52.26	1.68
Tap water 4	100	102.11	104.34	1.53
Landfill leachate 1	0	c	c	–
Landfill leachate 2	5.0	5.12	5.04	1.11
Landfill leachate 3	50.0	51.96	53.23	1.71
Landfill leachate 4	10.0	101.19	102.97	1.23

[c]No Pb^{2+} could be detected.
[a] Mean of three replicate measurements.
[b] SD=standard deviation.

4. Conclusion

In conclusion, a biosensor consisting of nanoporous gold (NPG), and GR–5DNAzyme with anionic intercalator was developed, which provided the potential to quantify trace levels of Pb^{2+} in environmental water samples. NPG, GR–5DNAzyme and the anionic intercalator improved the detection performance of the sensor significantly, and it exhibited satisfactory results for Pb^{2+} ion detection with high sensitivity and selectivity. This sensor exhibited relatively wide dynamic working ranges (1–120 nM) and detection limits (0.02 nM). It has good potential for application in real water monitoring. Furthermore, alternative sensing devices for other metal ions may be developed as well using other natural or synthetic hairpin probes.

Acknowledgments

The study was financially supported by Projects 51579096, 51222805, 51521006, 51679084 and 51508175 supported by National Natural Science Foundation of China, the National Program for Support of Top–Notch Young Professionals of China (2012), and the Program for New Century Excellent Talents in University from the Ministry of Education of China (NCET-11-0129). Project of Science and Technology of Hunan Province (2015WK3016 and 2016WK2010).

Appendix A. Supplementary material

Supplementary data associated with this article can be found in the online version at http://dx.doi.org/10.1016/j.talanta.2016.12.069.

References

[1] Y. Xiao, A.A. Rowe, K.W. Plaxo, Electrochemical detection of parts-per-billion lead via an electrode-bound DNAzyme assembly, J. Am. Chem. Soc. 129 (2) (2007) 262–263.
[2] X.H. Zhao, L. Gong, Y. Wu, X.B. Zhang, J. Xie, Cationic-perylene-G-quadruplex complex based fluorescent biosensor for label-free detection of Pb^{2+}, Talanta 149 (2016) 98–102.
[3] H. Sun, L. Yu, H. Chen, J. Xiang, X. Zhang, Y. Shi, Q. Yang, A. Guan, Q. Li, Y. Tang, A colorimetric lead(II) ions sensor based on selective recognition of G-quadruplexes by a clip-like cyanine dye, Talanta 136 (2015) 210–214.
[4] T. Fu, S. Ren, L. Gong, H. Meng, L. Cui, R.-M. Kong, X.-B. Zhang, W. Tan, A label-free DNAzyme fluorescence biosensor for amplified detection of Pb^{2+}-based on cleavage-induced G-quadruplex formation, Talanta 147 (2016) 302–306.
[5] S. Cerovac, V. Guzsvány, Z. Kónya, A.M. Ashrafi, I. Švancara, S. Rončević, Á. Kukovecz, B. Dalmacija, K. Vytřas, Trace level voltammetric determination of lead and cadmium in sediment pore water by a bismuth-oxychloride particle-multiwalled carbon nanotube composite modified glassy carbon electrode, Talanta 134 (2015) 640–649.
[6] D. Agustini, A.S. Mangrich, M.F. Bergamini, L.H. Marcolino-Junior, Sensitive voltammetric determination of lead released from ceramic dishes by using of bismuth nanostructures anchored on biochar, Talanta 142 (2015) 221–227.
[7] Y. Zhou, L. Tang, G. Zeng, C. Zhang, Y. Zhang, X. Xie, Current progress in biosensors for heavy metal ions based on DNAzymes/DNA molecules functionalized nanostructures: a review, Sens. Actuators B: Chem. 223 (2016) 280–294.
[8] Y. Wang, H. Ge, Y. Wu, G. Ye, H. Chen, X. Hu, Construction of an electrochemical sensor based on amino-functionalized metal-organic frameworks for differential pulse anodic stripping voltammetric determination of lead, Talanta 129 (2014) 100–105.
[9] D. Agustini, A.S. Mangrich, M.F. Bergamini, L.H. Marcolino-Junior, Sensitive voltammetric determination of lead released from ceramic dishes by using of bismuth nanostructures anchored on biochar, Talanta 142 (2015) 221–227.
[10] C.D. Palmer, M.E. Lewis, C.M. Geraghty, F. Barbosa, P.J. Parsons, Determination of lead, cadmium and mercury in blood for assessment of environmental exposure: a comparison between inductively coupled plasma–mass spectrometry and atomic absorption spectrometry, Spectrochim. Acta Part B At. Spectrosc. 61 (8) (2006) 980–990.
[11] V. Ettler, M. Mihaljevič, M. Komárek, ICP-MS measurements of lead isotopic ratios in soils heavily contaminated by lead smelting: tracing the sources of pollution, Anal. Bioanal. Chem. 378 (378) (2004) 311–317.
[12] M.L. Yola, N. Atar, M.S. Qureshi, Z. Üstünda, A.O. Solak, Electrochemically grafted etodolac film on glassy carbon for Pb(II) determination, Sens. Actuators B Chem. 171–172 (9) (2012) 1207–1215.
[13] L. Chen, Z. Li, Y. Meng, P. Zhang, Z. Su, Y. Liu, Y. Huang, Y. Zhou, Q. Xie, S. Yao, Sensitive square wave anodic stripping voltammetric determination of Cd^{2+} and Pb^{2+} ions at Bi/Nafion/overoxidized 2-mercaptoethanesulfonate-tethered polypyrrole/glassy carbon electrode, Sens. Actuators B Chem. 191 (2) (2014) 94–101.
[14] C. Zhang, Y. Zhou, L. Tang, G. Zeng, J. Zhang, B. Peng, X. Xie, C. Lai, B. Long, J. Zhu, Determination of Cd^{2+} and Pb^{2+} based on mesoporous carbon nitride/self-doped polyaniline nanofibers and square wave anodic stripping voltammetry, Nanomaterials 6 (1) (2016) 340–362.
[15] L. Tang, J. Chen, G. Zeng, Y. Zhu, Y. Zhang, Y. Zhou, X. Xie, G. Yang, S. Zhang, Ordered mesoporous carbon and thiolated polyaniline modified electrode for simultaneous determination of Cadmium(II) and Lead(II) by anodic stripping voltammetry, Electroanalysis 26 (10) (2014) 2283–2291.
[16] T. Lan, K. Furuya, Y. Lu, A highly selective lead sensor based on a classic lead DNAzyme, Chem. Commun. 46 (22) (2010) 3896–3898.
[17] J. Liu, A.K. Brown, X. Meng, D.M. Cropek, J.D. Istok, D.B. Watson, Y. Lu, A catalytic beacon sensor for uranium with parts-per-trillion sensitivity and millionfold selectivity, Proc. Natl. Acad. Sci. USA 104 (7) (2007) 2056–2061.
[18] M. Hollenstein, C. Hipolito, C. Lam, D. Dietrich, D.M. Perrin, A highly selective DNAzyme sensor for mercuric ions, Angew. Chem. Int. Ed. 47 (23) (2008) (4346-50).
[19] L. Jing, L. Yi, A highly sensitive and selective catalytic DNA biosensor for lead ions, J. Am. Chem. Soc. 122 (42) (2000) 10466–10467.
[20] J.H. Lee, Z. Wang, J. Liu, Y. Lu, Highly sensitive and selective colorimetric sensors for uranyl (UO_2^{2+}): development and comparison of labeled and label-free DNAzyme-gold nanoparticle systems, J. Am. Chem. Soc. 130 (43) (2008) 14217–14226.
[21] W. Wang, L.P. Billen, Y. Li, Sequence diversity, metal specificity, and catalytic proficiency of metal-dependent phosphorylating DNA enzymes, Chem. Biol. 9 (4) (2002) 507–517.
[22] S.W. Santoro, G.F. Joyce, K. Sakthivel, S. Gramatikova, RNA cleavage by a DNA enzyme with extended chemical functionality, J. Am. Chem. Soc. 122 (11) (2000) 2433–2439.
[23] J. Liu, Y. Lu, Colorimetric Cu^{2+} detection with a ligation DNAzyme and nanoparticles, Chem. Commun. 68 (46) (2007) 4872–4874.
[24] W. Zhou, Y. Zhang, J. Ding, J. Liu, In Vitro selection in serum: rna-cleaving DNAzymes for measuring Ca^{2+} and Mg^{2+}, ACS Sens. 1 (5) (2016) 600–606.
[25] R. Saran, J. Liu, A silver DNAzyme, Anal. Chem. 88 (7) (2016) 4014–4020.
[26] P.J.J. Huang, M. Vazin, J. Liu, Desulfurization activated phosphorothioate DNAzyme for the detection of thallium, Anal. Chem. 87 (20) (2015) 10443–10449.
[27] P.J.J. Huang, J. Liu, Sensing parts-per-trillion Cd^{2+}, Hg^{2+}, and Pb^{2+} collectively and individually using phosphorothioate DNAzymes, Anal. Chem. 86 (12) (2014) 5999–6005.
[28] R. Saran, J.W. Liu, A comparison of two classic Pb^{2+}-dependent RNA-cleaving DNAzymes, Inorg. Chem. Front. 3 (2016) 494–501.
[29] L. Tang, G.M. Zeng, G.L. Shen, Y.P. Li, Y. Zhang, D.L. Huang, Rapid detection of picloram in agricultural field samples using a disposable immunomembrane-based electrochemical sensor, Environ. Sci. Technol. 42 (4) (2008) 1207–1212.
[30] Y. Zhou, T. Lin, G. Zeng, J. Chen, J. Wang, C. Fan, G. Yang, Z. Yi, X. Xia, Amplified and selective detection of manganese peroxidase genes based on enzyme-scaffolded-gold nanoclusters and mesoporous carbon nitride, Biosens. Bioelectron. 65C (2014) 382–389.
[31] Y. Zhou, T. Lin, G. Zeng, J. Chen, C. Ye, Z. Yi, G. Yang, Y. Liu, Z. Chen, W. Tang, Mesoporous carbon nitride based biosensor for highly sensitive and selective analysis of phenol and catechol in compost bioremediation, Biosens. Bioelectron. 61 (1) (2014) 519–525.
[32] Y. Zhou, T. Lin, G. Zeng, Z. Chen, X. Xia, Y. Liu, J. Wang, T. Jing, Z. Yi, Y. Deng, Label free detection of lead using impedimetric sensor based on ordered mesoporous carbon–gold nanoparticles and DNAzyme catalytic beacons, Talanta 146 (2016) 641–647.
[33] J. Yao, J. Li, J. Owens, W. Zhong, Combing DNAzyme with single-walled carbon nanotubes for detection of Pb(II) in water, Analyst 136 (4) (2011) 764–768.
[34] Y. Zhang, G.M. Zeng, L. Tang, D.L. Huang, X.Y. Jiang, Y.N. Chen, A hydroquinone biosensor using modified core–shell magnetic nanoparticles supported on carbon paste electrode, Biosens. Bioelectron. 22 (9–10) (2007) 2121–2126.
[35] Y. Luo, Y. Zhang, L. Xu, L. Wang, G. Wen, A. Liang, Z. Jiang, Colorimetric sensing

of trace UO_2^{2+} by using nanogold-seeded nucleation amplification and label-free DNAzyme cleavage reaction, Analyst 137 (8) (2012) 1866–1871.
[36] Y. Zhu, G.M. Zeng, Y. Zhang, L. Tang, J. Chen, M. Cheng, L.H. Zhang, L. He, Y. Guo, X.X. He, Highly sensitive electrochemical sensor using a MWCNTs/GNPs-modified electrode for lead(II) detection based on Pb^{2+}-induced G-rich DNA conformation, Analyst 139 (19) (2014) 5014–5020.
[37] X. Yang, J. Xu, X. Tang, H. Liu, D. Tian, A novel electrochemical DNAzyme sensor for the amplified detection of Pb^{2+} ions, Chem. Commun. 46 (18) (2010) 3107–3109.
[38] Y. Zhou, A novel biosensor for silver(I) ion detection based on nanoporous gold and duplex-like, DNA scaffolds anionic Inter., Rsc Adv. 5 (85) (2015) 69738–69744.
[39] C. Zhang, C. Lai, G. Zeng, D. Huang, L. Tang, C. Yang, Y. Zhou, L. Qin, M. Cheng, Nanoporous Au-based chronocoulometric aptasensor for amplified detection of Pb^{2+} using DNAzyme modified with Au nanoparticles, Biosens. Bioelectron. 81 (2016) 61–67.
[40] E.L.S. Wong, P. Erohkin, J.J. Gooding, A comparison of cationic and anionic intercalators for the electrochemical transduction of DNA hybridization via long range electron transfer, Electrochem. Commun. 6 (7) (2004) 648–654.
[41] G. Zeng, C. Zhang, D. Huang, C. Lai, L. Tang, Y. Zhou, P. Xu, H. Wang, L. Qin, M. Cheng, Practical and regenerable electrochemical aptasensor based on nanoporous gold and thymine-Hg2+-thymine base pairs for Hg2+ detection, Biosens. Bioelectron. 90 (2017) 542–548.
[42] J. Zhuang, L. Fu, M. Xu, Z. Qian, G. Chen, D. Tang, DNAzyme-based magneto-controlled electronic switch for picomolar detection of lead(II) coupling with DNA-based hybridization chain reaction, Biosens. Bioelectron. 45 (2) (2013) 52–57.
[43] L. Shen, Z. Chen, Y. Li, S. He, S. Xie, X. Xu, Z. Liang, X. Meng, Q. Li, Z. Zhu, Electrochemical DNAzyme sensor for lead based on amplification of DNA-Au bio-bar codes, Anal. Chem. 80 (16) (2008) 6323–6328.
[44] H. Zhang, B. Jiang, Y. Xiang, J. Su, Y. Chai, R. Yuan, DNAzyme-based highly sensitive electronic detection of lead via quantum dot-assembled amplification labels, Biosens. Bioelectron. 28 (1) (2011) 135–138.
[45] Y. Wang, J. Irudayaraj, A. SERS DNAzyme, biosensor for lead ion detection, Chem. Commun. 47 (47) (2011) 4394–4396.
[46] J. Zhu, Colorimetric detection of lead(II) ions based on accelerating surface etching of gold nanorods to nanospheres: the effect of sodium thiosulfate, Rsc Adv. 6 (2016) 25611–25619.
[47] D. Nie, H. Wu, Q. Zheng, L. Guo, P. Ye, Y. Hao, Y. Li, F. Fu, Y. Guo, A sensitive and selective DNAzyme-based flow cytometric method for detecting Pb^{2+} ions, Chem. Commun. 48 (8) (2012) 1150–1152.
[48] M. Liu, X. Lou, J. Du, M. Guan, J. Wang, X. Ding, J. Zhao, DNAzyme-based fluorescent microarray for highly selective and sensitive detection of lead(II), Analyst 137 (1) (2012) 70–82.
[49] R.I. Stefan, S.G. Bairu, Diamond paste based electrodes for the determination of Pb(II) at trace concentration levels, Talanta 63 (3) (2004) 605–608.
[50] K. Hamsawahini, P. Sathishkumar, R. Ahamad, A.R.M. Yusoff, PVDF–ErGO–GRC electrode: a single setup electrochemical system for separation, pre-concentration and detection of lead ions in complex aqueous samples, Talanta 148 (2016) 101–107.
[51] D. Huang, C. Niu, M. Ruan, X. Wang, G. Zeng, C. Deng, Highly sensitive strategy for Hg^{2+} detection in environmental water samples using long lifetime fluorescence quantum dots and gold nanoparticles, Environ. Sci. Technol. 47 (9) (2013) 4392–4398.